






III Science, Technology, and Innovation Fair of UFSM-CS

Stabilization control of the inverted pendulum on a self-balancing cart

Controle de estabilização do pêndulo invertido em um carro de autoequilíbrio

Pedro Henrique Cascardo Cabral¹ , **André Francisco Caldeira**¹ ,
Charles Rech¹ , **Simone Ferigolo Venturini**² , **Cristiano Frandalozo Maidana**¹ ,
Carmen Brum Rosa² 

¹Federal University of Santa Maria, Cachoeira do Sul, RS, Brazil

²Federal University of Santa Maria, Santa Maria, RS, Brazil

ABSTRACT

The inverted pendulum is one of the most challenging systems in control theory, serving as a key model for real-world applications that require dynamic balance, such as biped robots, autonomous vehicles, and aerospace systems. Its highly nonlinear, unstable, and underactuated nature poses significant challenges, demanding advanced control strategies. This study adopts the inverted pendulum system on a self-balancing cart as the object of analysis, conducting a dynamic study based on Lagrangian mechanics to derive the equations of motion, which are later reformulated into state-space form. For the stabilization phase, the Linear Quadratic Regulator (LQR) is employed, offering advantages such as full-state feedback, minimal control effort, fast settling time, and smooth system response, characteristics obtained through the minimization of a cost function assigned to each state and control variable. This work proposes an effective methodology for modeling, linearization, and control of nonlinear dynamic systems, applied to an inverted pendulum mounted on a self-balancing cart, aimed at applications in autonomous systems, robotics, electrical engineering, mechanical engineering, and aerospace engineering.

Keywords: Inverted pendulum; Self-balancing cart; LQR controller; Nonlinear control systems; Dynamic stabilization

RESUMO

O pêndulo invertido representa um dos sistemas mais desafiadores da teoria de controle, servindo como um modelo-chave para aplicações reais que exigem equilíbrio dinâmico, como robôs bípedes, veículos autônomos e sistemas aeroespaciais. Sua natureza altamente não linear, instável e subatuada impõe desafios significativos, exigindo estratégias de controle avançadas. Este trabalho adota o sistema de pêndulo invertido sobre um carrinho de autoequilíbrio como objeto de estudo, realizando uma análise dinâmica baseada na mecânica lagrangiana para a obtenção das equações de movimento, posteriormente reescritas na forma de espaço de estados. Para a fase de estabilização, empregou-se o Regulador Linear Quadrático (LQR), que oferece vantagens como realimentação de estado completo, esforço de controle mínimo, tempo de assentamento rápido e resposta suave do sistema, obtidas através da minimização de uma função de custo atribuída a cada variável de estado e de controle. Por meio deste estudo, propõe-se uma metodologia eficaz para modelagem, linearização e controle de sistemas dinâmicos não lineares, aplicado a um pêndulo invertido montado em um carro de autoequilíbrio, visando aplicações em sistemas autônomos, robótica, engenharia elétrica, engenharia mecânica e engenharia aeroespacial.

Palavras-chave: Pêndulo invertido; Carrinho de autoequilíbrio; Controlador LQR; Sistemas de controle não lineares; Estabilização dinâmica

1 INTRODUCTION

The inverted pendulum is one of the most challenging and widely studied classical systems in control theory. According to (Stimac, 1999), the interest in studying this type of system is not only due to the variety of techniques that can be applied for its stabilization, but also to its usefulness as a representative model for several real-world systems that require dynamic balance, such as the movement of robots, autonomous vehicles, and even aerospace systems (Anderson, 1989; Huang and Huang, 1994; Nise, 2013; Ogata, 2011). In simple terms, its structure consists of a motor-driven cart (moving base) with a metal rod mounted at the top, as illustrated in 1), and it has two degrees of freedom: the horizontal translation of the cart and the rotation of the rod about its upper mounting point (Bugeja, 2003). According to (Bugeja, 2003), the inverted pendulum is a highly nonlinear, unstable, and underactuated system, which makes it ideal for the development of various classical and modern control techniques. These characteristics make its control a significant research field in various areas, such as electrical engineering, mechanical engineering, control and automation engineering, as well as aerospace engineering.

This inherent complexity is primarily due to the system's nonlinearity, which refers to the fact that its dynamic behavior changes depending on its current state. According to (Nise, 2013), this means that the system's response does not follow a proportional or predictable relationship between inputs and outputs throughout its entire operating range. Small variations in initial conditions can lead to completely different responses, making the control more complex. Unlike linear systems, where it is possible to accurately predict how the system will react to a command, nonlinear systems such as the inverted pendulum require more sophisticated and adaptive controllers, especially when operating away from the equilibrium point.

In addition to nonlinearity, the instability of the system is also a key factor. It is associated with the equilibrium configuration of the pendulum in the upright position, which is naturally unstable, as the natural position of the pendulum is downward due to the action of gravity pulling it in that direction (Santos, 2022). Small disturbances caused by external forces, sensor noise, or inaccuracies in the mathematical model can quickly drive the pendulum away from the desired position, which is the upright position, requiring continuous and precise control actions to maintain stability.

Another challenge that arises in this system is its underactuated nature. The system has eight state variables that describe its dynamics and only two control inputs. This means that, although the system has a larger number of variables that describe its behavior, the available control inputs are insufficient to influence all of them independently. Since the force used to control the rod is applied to the cart, not directly to the rod itself, the system is said to be underactuated (Santos, 2022). As a result, control strategies must take into account the dynamic coupling between the states, using advanced techniques to ensure stabilization and control objectives, even without the possibility of directly controlling each individual state.

Building on this foundation, in this work, the inverted pendulum system on a self-balancing cart is adopted as the object of study. Initially, a dynamic analysis based on Lagrangian mechanics is performed, which allows the precise formulation of the system's equations from its kinetic and potential energy. Subsequently, these equations are rewritten in state-space form, with the aid of block matrix operations, thus preparing the model for the design and simulation of modern controllers.

In the search for effective control solutions, several approaches have been explored in the literature for controlling systems of this nature. Energy and passivity-based techniques, for example, are effective during the "swing-up" phase (Åström and Furuta, 2000) which is the process of moving the pendulum from the stable lower position to the unstable upright position. This movement involves applying forces that make the pendulum swing in a controlled manner, gaining enough energy to reach the upright position. Alternative methods, such as fuzzy control and adaptive control, have also been successfully applied, particularly due to their ability to handle the system's nonlinearity and complexity without requiring precise mathematical models. Adaptive control, for instance, has been effectively used to address time-varying uncertainties in inverted pendulum systems, demonstrating robust performance in nonlinear dynamic environments (Chen and Huang, 2014). Fuzzy control is especially useful for designing controllers based on heuristic rules, avoiding complex analytical calculations (Eini and Abdelwahed, 2019).

For the stabilization phase, when the pendulum is already near the vertical position, the use of the Linear Quadratic Regulator (LQR) stands out as offering an optimal solution that balances control effort and tracking error. The LQR is based on full-state feedback and is capable of ensuring a fast settling time, a smooth response, and zero steady-state error (Kumar and Jerome, 2013). This paper, after a brief conceptual review of the LQR controller, proposes its application in the stabilization control of the inverted pendulum system on a self-balancing cart.

Thus, this study integrates both theoretical and practical aspects in the control of nonlinear dynamic systems, proposing an effective methodology for modeling, linearization, and control, with a view to future applications in autonomous systems, robotics, and aerospace engineering.

2 Mathematical Model

In this part of establishing the mathematical model, we conduct a dynamic analysis of the balanced cart inverted pendulum (Figure 1) based on Lagrangian mechanics, solving for the state space expression of the system.

Figure 1 – Physical image of the balanced car inverted pendulum



Source: <https://wheeltec.net>

2.1 Lagrangian mechanics

Lagrangian mechanics is an alternative formulation of Newtonian mechanics that describes the behavior of physical systems based on energy-derived principles and variational calculus (Lynch and Park, 2017; Taylor, 2005). Developed by Joseph-Louis Lagrange in the 18th century, this approach stands out for its effectiveness in modeling systems with three or fewer degrees of freedom and constraints (Lynch and Park, 2017; Taylor, 2005). The method is based on the definition of a scalar function called the Lagrangian (L), which represents the difference between the system's kinetic energy (T) and potential energy (V), as shown in Equation (1), instead of relying on forces and torques as in Newtonian mechanics (Taylor, 2005).

$$L = T - V. \quad (1)$$

This approach is based on the principle of least action, also known as Hamilton's principle, which asserts that the actual trajectory of a system is the one that makes the action stationary, typically minimizing it. The action is defined as the integral of the Lagrangian over time, as shown in Equation (2) below (Alves, 2017; Taylor, 2005):

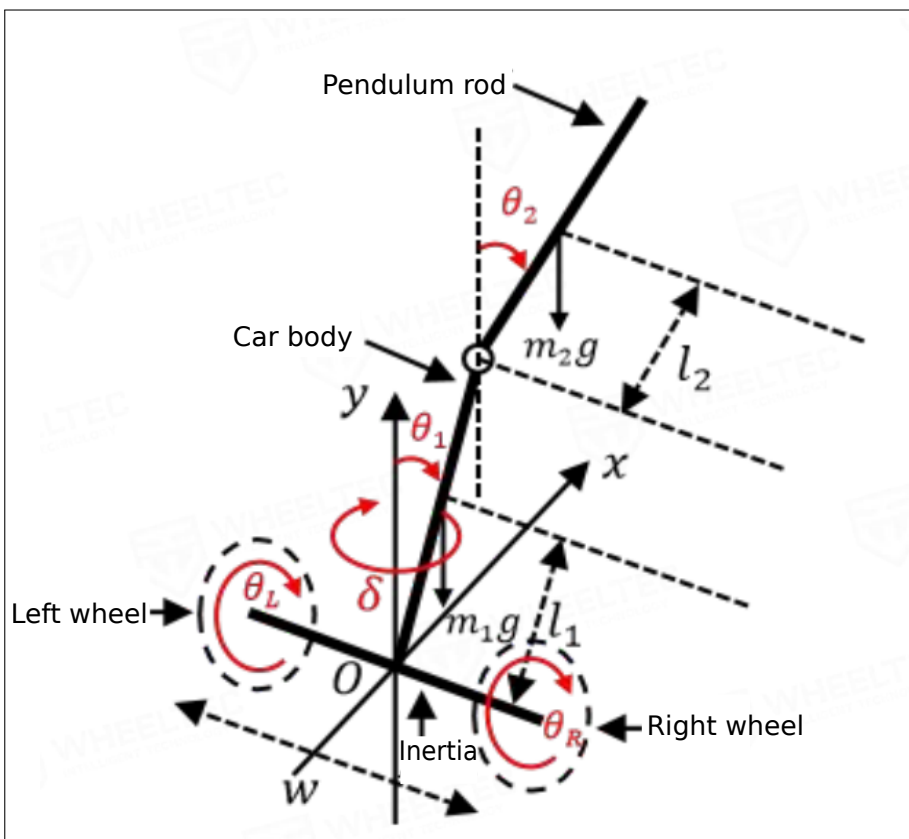
$$S = \int_{t_1}^{t_2} L dt, \quad (2)$$

where S represents the action of the system, t_1 is the initial time and t_2 is the final time of the trajectory under consideration. Applying this principle leads to the Euler-Lagrange equations, which describe the dynamics of the system (Alves, 2017).

2.2 Balanced cart inverted pendulum model

To facilitate the analysis, we can simplify the inverted pendulum model of the balancing car. Assume that the left and right wheels are exactly the same (radius, mass, moment of inertia). Ignoring air resistance, the inverted pendulum of the balancing car can be regarded as a system consisting of wheels and a pendulum rod. The simplified model and the adopted rectangular coordinate system are shown in Figure 2, with the corresponding symbols defined in Table 1.

Figure 2 – Inverted pendulum model of a balancing car



Source: <https://wheeltec.net>

Table 1 – Symbol Description

Inverted pendulum of the balancing car	
Parameter	Description and default measurement unit
m_1	Mass of the vehicle body (kg)
m_2	Mass of the pendulum rod (kg)
m_{wheel}	Mass of wheel (kg)
θ_L	Left wheel rotation angle (rad)
θ_R	Right wheel rotation angle (rad)
θ_1	The inclination angle of the vehicle body (rad)
θ_2	The inclination angle of the pendulum (rad)
l_1	Distance from the center of mass of the vehicle to the axis of rotation 1 (m)
l_2	Distance from the center of mass of the vehicle to the axis of rotation 2 (m)
L_1	The length of the car body (m)
L_2	Length of the pendulum (m)
w	Wheelbase (m)
r	Radius of wheel (m)
I_{wheel}	The moment of inertia of the wheel when it rotates ($kg \cdot m^2$)
I_1	The moment of inertia of the vehicle body when it rotates around its center of mass ($kg \cdot m^2$)
I_2	The moment of inertia of the pendulum when it rotates around its center of mass ($kg \cdot m^2$)
J_δ	The moment of inertia of the vehicle body when it rotates ($kg \cdot m^2$)

Source: Authors

After defining the physical parameters and establishing the coordinate system, we proceed with the mathematical modeling of the system's energy components. In the context of Lagrangian mechanics, both the translational and rotational kinetic energies must be accounted for when analyzing the dynamics of the balancing car. Since the left and right wheels are assumed to be identical, it is sufficient to derive the expression for one of them.

The kinetic energy of the left wheel is composed of two components: the translational kinetic energy due to the wheel's linear motion and the rotational kinetic energy due to its spinning. The total kinetic energy of the left wheel is given by:

$$E_{kL} = \frac{r^2}{2} m_{wheel} \dot{\theta}_L^2 + \frac{1}{2} I_{wheel} \dot{\theta}_L^2.$$

In addition to the kinetic energies, the potential energy of the system must also be considered, which arises from the interaction of the left wheel with gravity. The potential energy is associated with the vertical position of the center of mass of the left

wheel relative to the reference point. In the case of the simplified model, the potential energy of the left wheel can be expressed as:

$$E_{pL} = 0.$$

Moving on to the right wheel, its kinetic energy follows a similar structure. Like the left wheel, the right wheel's kinetic energy consists of two components: translational kinetic energy and rotational kinetic energy. Together, these two contributions account for the total kinetic energy of the right wheel, which is given by:

$$E_{kR} = \frac{r^2}{2} m_{wheel} \dot{\theta}_R^2 + \frac{1}{2} I_{wheel} \dot{\theta}_R^2.$$

After discussing the kinetic energy of the right wheel, we now turn to its potential energy. Similar to the left wheel, the potential energy of the right wheel arises from the effect of gravity. This energy is determined by the vertical displacement of the right wheel's center of mass relative to the reference point. In the simplified model, the potential energy associated with the right wheel is given by:

$$E_{pR} = 0.$$

The displacement of the vehicle body is fundamental for describing the overall motion of the system. It is defined by the positions in the x and y directions and is influenced by both the rotational movements of the left and right wheels, as well as the rotation of the vehicle body itself. These contributions are combined into a single expression that reflects the net displacement of the system and forms the basis for energy calculations as can be seen in the Equation (3) below. In the simplified model, the total displacement of the vehicle body is given by:

$$\begin{cases} x_1 = \frac{r}{2} (\theta_L + \theta_R) + l_1 \sin \theta_1 \\ y_1 = l_1 \cos \theta_1. \end{cases} \quad (3)$$

Building upon this, the velocity of the vehicle body is a combination of the velocities of the left and right wheels and the rotation of the vehicle body. These

velocities are essential for determining the kinetic energy of the vehicle body, reflecting the motion and interaction between the wheels and the vehicle body. The components \dot{x}_1 and \dot{y}_1 represent the rate of change of the vehicle's displacement in the x and y directions, respectively, as described by Equation (4) below.

$$\begin{cases} \dot{x}_1 = \frac{r}{2} (\dot{\theta}_L + \dot{\theta}_R) + \dot{\theta}_1 l_1 \cos \theta_1 \\ \dot{y}_1 = -\dot{\theta}_1 l_1 \sin \theta_1. \end{cases} \quad (4)$$

The kinetic energy of the vehicle body, given by Equation (5) below, considers both the translational and rotational motion of the body. It is influenced by the rotations of the wheels and the rotation of the vehicle body itself.

$$\begin{aligned} E_{k1} = & \frac{r^2}{8} m_1 (\dot{\theta}_L + \dot{\theta}_R)^2 + \frac{1}{2} (m_1 l_1^2 + I_1) \dot{\theta}_1^2 \\ & + \frac{r}{2} m_1 l_1 (\dot{\theta}_L + \dot{\theta}_R) \dot{\theta}_1 \cos \theta_1 + \frac{1}{2} J_\delta \left(\frac{\dot{\theta}_L + \dot{\theta}_R}{w} \right)^2. \end{aligned} \quad (5)$$

The potential energy of the vehicle body arises due to its height relative to a fixed reference level, typically considered the ground. This energy depends on the mass of the body, gravitational acceleration, and its vertical position determined by the angle θ_1 , as shown in Equation (6) below.

$$E_{p1} = m_1 g l_1 \cos \theta_1. \quad (6)$$

To continue the analysis, the displacement of the pendulum is introduced. This displacement is influenced not only by the rotation of the wheels but also by the orientation of the vehicle body and the pendulum itself. As detailed in Equation (7), the pendulum's position in both the x and y directions is expressed by summing the contributions from each of these rotational effects.

$$\begin{cases} x_2 = \frac{r}{2} (\theta_L + \theta_R) + L_1 \sin \theta_1 + l_2 \sin \theta_2 \\ y_2 = L_1 \cos \theta_1 + l_2 \cos \theta_2. \end{cases} \quad (7)$$

The pendulum's velocity results from the combined motion of the wheels, the rotation of the vehicle body, and the pendulum's own swing. These velocities are crucial

for calculating the kinetic energy of the pendulum. These components are expressed in Equation (8), where the time derivatives of the angular displacements describe how quickly the pendulum moves in each direction.

$$\begin{cases} \dot{x}_2 = \frac{r}{2} (\dot{\theta}_L + \dot{\theta}_R) + \dot{\theta}_1 L_1 \cos \theta_1 + \dot{\theta}_2 l_2 \cos \theta_2 \\ \dot{y}_2 = -\dot{\theta}_1 L_1 \sin \theta_1 - \dot{\theta}_2 l_2 \sin \theta_2. \end{cases} \quad (8)$$

With the velocity expressions established, the kinetic energy of the pendulum can be determined. This energy includes terms associated with translational motion from the wheel rotation, rotational motion of both the body and pendulum, and their interactions, as shown in Equation (9) below.

$$\begin{aligned} E_{k2} = & \frac{r^2}{8} m_2 (\dot{\theta}_L + \dot{\theta}_R)^2 + \frac{1}{2} m_2 L_1^2 \dot{\theta}_1^2 + \frac{1}{2} (m_2 l_2^2 + I_2) \dot{\theta}_2^2 \\ & + \frac{r}{2} m_2 L_1 (\dot{\theta}_L + \dot{\theta}_R) \dot{\theta}_1 \cos \theta_1 + \frac{r}{2} m_2 l_2 (\dot{\theta}_L + \dot{\theta}_R) \dot{\theta}_2 \cos \theta_2 \\ & + m_2 L_1 l_2 \dot{\theta}_1 \dot{\theta}_2 \cos (\theta_1 - \theta_2). \end{aligned} \quad (9)$$

In addition to its kinetic energy, the pendulum also possesses potential energy due to gravity. This energy depends on the mass of the pendulum and its height, which varies with the angles θ_1 and θ_2 , as presented in Equation (10):

$$E_{p2} = m_2 g L_1 \cos \theta_1 + m_2 g l_2 \cos \theta_2. \quad (10)$$

Combining all the kinetic energy components, Equation (11) provides the total kinetic energy of the system. This includes the contributions from the wheels, the vehicle body, and the pendulum, accounting for both individual and coupled motions.

$$\begin{aligned}
 T &= E_{kL} + E_{kR} + E_{k1} + E_{k2} \\
 &= \left(\frac{r^2}{2} m_{wheel} + \frac{1}{2} I_{wheel} \right) (\dot{\theta}_L + \dot{\theta}_R)^2 + \frac{r^2}{8} (m_1 + m_2) (\dot{\theta}_L + \dot{\theta}_R)^2 + \frac{1}{2} J_\delta \left(\frac{\dot{\theta}_L + \dot{\theta}_R}{w} \right)^2 \\
 &+ \left(\frac{r}{2} m_1 l_1 \dot{\theta}_1 \cos \theta_1 + \frac{r}{2} m_2 L_1 \dot{\theta}_1 \cos \theta_1 + \frac{r}{2} m_2 l_2 \dot{\theta}_2 \cos \theta_2 \right) (\dot{\theta}_L + \dot{\theta}_R) \\
 &+ \frac{1}{2} (m_1 l_1^2 + m_2 L_1^2 + I_1) \dot{\theta}_1^2 + \frac{1}{2} (m_2 l_2^2 + I_2) \dot{\theta}_2^2 \\
 &+ m_2 L_1 l_2 \dot{\theta}_1 \dot{\theta}_2 \cos (\theta_1 - \theta_2).
 \end{aligned} \tag{11}$$

The expression for the total potential energy of the system is presented in Equation (12). It combines the gravitational potential energy of the left and right wheels, the vehicle body, and the pendulum.

$$V = E_{pL} + E_{pR} + E_{p1} + E_{p2} = (m_1 l_1 + m_2 L_1) g \cos \theta_1 + m_2 g l_2 \cos \theta_2. \tag{12}$$

With the expressions for both the total kinetic energy and the total potential energy of the system fully defined, the Lagrangian function L can now be obtained as the difference between T and V . This scalar function encapsulates the dynamic behavior of the system by incorporating the contributions of all relevant masses, their velocities, and their positions under gravitational influence. The resulting Lagrangian, expressed in Equation (13), serves as the foundation for deriving the equations of motion that govern the system's dynamics.

$$\begin{aligned}
 L &= T - V \\
 &= \left(\frac{r^2}{2} m_{wheel} + \frac{1}{2} I_{wheel} \right) (\dot{\theta}_L + \dot{\theta}_R)^2 + \frac{r^2}{8} (m_1 + m_2) (\dot{\theta}_L + \dot{\theta}_R)^2 + \frac{1}{2} J_\delta \left(\frac{\dot{\theta}_L + \dot{\theta}_R}{w} \right)^2 \\
 &+ \left(\frac{r}{2} m_1 l_1 \dot{\theta}_1 \cos \theta_1 + \frac{r}{2} m_2 L_1 \dot{\theta}_1 \cos \theta_1 + \frac{r}{2} m_2 l_2 \dot{\theta}_2 \cos \theta_2 \right) (\dot{\theta}_L + \dot{\theta}_R) \\
 &+ \frac{1}{2} (m_1 l_1^2 + m_2 L_1^2 + I_1) \dot{\theta}_1^2 + \frac{1}{2} (m_2 l_2^2 + I_2) \dot{\theta}_2^2 + m_2 L_1 l_2 \dot{\theta}_1 \dot{\theta}_2 \cos (\theta_1 - \theta_2) \\
 &- (m_1 l_1 + m_2 L_1) g \cos \theta_1 - m_2 g l_2 \cos \theta_2.
 \end{aligned} \tag{13}$$

With the total kinetic and potential energies defined, the next step is to formulate the Euler-Lagrange equations of motion for the system, which is given by:

$$\frac{d}{dt} \left(\frac{\partial L}{\partial \dot{q}} \right) = Q_{non-conservative},$$

where: q is the generalized coordinate, describing the system's configuration along a specific degree of freedom and characterizing the position or displacement of the component under analysis; \dot{q} is the generalized velocity, defined as the time derivative of the generalized coordinate, describing the rate of change of the system's configuration over time and playing a key role in characterizing its kinetic energy; and $Q_{non-conservative}$ is the generalized non-conservative force accounting for energy dissipation mechanisms such as friction, air resistance, and other forces that do not conserve mechanical energy. These forces contribute to the total virtual work but cannot be derived from a potential energy function.

With the Lagrangian function defined, the next step is to apply the Euler-Lagrange formalism to derive the equations of motion for the system. This process involves selecting appropriate generalized coordinates that describe the system's configuration, in this case, the angular displacements θ_1 and θ_2 . For each generalized coordinate, the Euler-Lagrange equation is applied individually.

By assigning $q_1 = \theta_1$, which represents the angular displacement of the vehicle body, we derive the corresponding equation of motion:

$$\begin{aligned} & \frac{r}{2} (m_1 l_1 + m_2 L_1) \cos \theta_1 \left(\ddot{\theta}_L + \ddot{\theta}_R \right)^2 + (m_1 l_1^2 + m_2 L_1^2 + I_1) \ddot{\theta}_1 \\ & + m_2 L_1 l_2 \ddot{\theta}_2 \cos \theta_1 (\theta_1 - \theta_2) + m_2 L_1 l_2 \dot{\theta}_2^2 \sin (\theta_1 - \theta_2) \\ & - (m_1 l_1 + m_2 L_1) g \sin \theta_1 = 0. \end{aligned}$$

Following the same procedure, by defining $q_2 = \theta_2$, which corresponds to the angular displacement of the pendulum, we derive the second equation of motion that captures its dynamics:

$$\frac{r}{2}m_2l_2 \cos \theta_2 \left(\ddot{\theta}_L + \ddot{\theta}_R \right) + (m_2l_2^2 + I_2)\ddot{\theta}_2 + m_2L_1l_2\ddot{\theta}_1 \cos (\theta_1 - \theta_2) - m_2L_1l_2 \sin (\theta_1 - \theta_2) \dot{\theta}_1^2 - m_2gl_2 \sin \theta_2 = 0.$$

2.3 Linearization

As the system of equations contains nonlinear terms, it is necessary to linearize it. A system is classified as nonlinear when it does not satisfy the superposition principle, meaning its response to multiple inputs cannot be obtained by summing the individual responses to each input applied separately (Ogata, 2011).

The principle of superposition is a fundamental property of linear systems. It states that, for a system to be considered linear, it must simultaneously satisfy two conditions, which are presented below.

Additivity: If the input $\mathbf{u}_1(t)$ produces the output $\mathbf{y}_1(t)$, and the input $\mathbf{u}_2(t)$ produces the output $\mathbf{y}_2(t)$, then the combined input $\mathbf{u}(t) = \mathbf{u}_1(t) + \mathbf{u}_2(t)$ must produce the combined output $\mathbf{y}(t) = \mathbf{y}_1(t) + \mathbf{y}_2(t)$.

Homogeneity (or Scalability): If the input $\mathbf{u}(t)$ produces the output $\mathbf{y}(t)$, then the input scaled by a constant α , that is $\alpha\mathbf{u}(t)$ must produce the output $\alpha\mathbf{y}(t)$.

If both conditions are satisfied, the system is said to obey the principle of superposition and is therefore classified as linear. In the case of the inverted pendulum system on a self-balancing cart, the principle of superposition is not satisfied, therefore, the system is characterized as nonlinear.

Considering the inclination angle of the stabilizer bar (car body) is relatively small (usually, $-10^\circ \leq \theta_{1,2} \leq 10^\circ$), it can be considered that:

$$\begin{cases} \cos \theta_{1,2} = 1 \\ \sin \theta_{1,2} = 0 \\ \dot{\theta}_{1,2}^2 = 0. \end{cases}$$

So the equation system becomes:

$$\begin{cases} \frac{r}{2}(m_1 l_1 + m_2 L_1) \ddot{\theta}_L + \frac{r}{2}(m_1 l_1 + m_2 L_1) \ddot{\theta}_R + (m_1 l_1^2 + m_2 L_1^2 + I_1) \ddot{\theta}_1 \\ + m_2 L_1 l_2 \ddot{\theta}_2 = (m_1 l_1 + m_2 L_1) g \theta_1 \\ \frac{r}{2} m_2 l_2 \ddot{\theta}_L + \frac{r}{2} m_2 l_2 \ddot{\theta}_R + m_2 L_1 l_2 \ddot{\theta}_1 + (m_2 l_2^2 + I_2) \ddot{\theta}_2 = m_2 g l_2 \theta_2. \end{cases} \quad (14)$$

The Equation (14) is the dynamic equation of the inverted pendulum of the balancing car.

2.4 State-Space Expression

The state-space formulation serves as the foundation of modern control theory and provides a structured and flexible framework for modeling, analyzing, and designing dynamic systems. This approach describes the system through a set of first-order differential equations that capture both its internal dynamics and input-output relationships, which can be combined into a first-order vector-matrix differential equation (Ogata, 2011).

Unlike classical techniques, that often rely on transfer functions and are limited to single-input single-output (SISO) systems, the state space method is particularly advantageous for multi-input multi-output (MIMO) systems, as well as systems that are time-varying or nonlinear (Nise, 2013; Ogata, 2011). By defining appropriate state variables, the dynamic behavior of the system can be expressed in a vector-matrix notation, simplifying the mathematical representation of the system of equations, facilitating simulations, control design, and stability analysis.

To formulate a system in the state-space representation, it is necessary to define a state vector $\mathbf{x}(t)$, an input vector $\mathbf{u}(t)$, and an output vector $\mathbf{y}(t)$. The general form of a continuous-time linear time-invariant (LTI) system is described by the following set of equations:

$$\begin{cases} \mathbf{x}(t) = \mathbf{A}\mathbf{x}(t) + \mathbf{B}\mathbf{u}(t) \\ \mathbf{y}(t) = \mathbf{C}\mathbf{x}(t) + \mathbf{D}\mathbf{u}(t). \end{cases}$$

in this formulation: $\mathbf{x}(t) \in \mathbb{R}^n$ is the state vector containing the internal variables of the system, which capture its dynamic behavior over time, summarizing the past inputs and states that influence the system's future evolution; $\mathbf{u}(t) \in \mathbb{R}^m$ is the input vector, representing external control signals or disturbances applied to the system; $\mathbf{y}(t) \in \mathbb{R}^p$ is the output vector, which contains the measured or observed quantities that result from the system's internal state and input; $\mathbf{A} \in \mathbb{R}^{n \times n}$ is the state matrix, defining how the current state influences its own rate of change; $\mathbf{B} \in \mathbb{R}^{n \times m}$ is the input matrix, determining how the inputs affect the state dynamics; $\mathbf{C} \in \mathbb{R}^{p \times n}$ is the output matrix, describing how the state variables contribute to the output; and $\mathbf{D} \in \mathbb{R}^{p \times m}$ is the feedthrough (or direct transmission) matrix, representing any direct influence of the inputs on the outputs, independent of the state.

These equations form the foundation for expressing dynamic systems in a compact and structured manner, which is especially useful for computer-based simulations and controller synthesis. In this subsection, the system under study is rewritten using the state space representation, providing a solid foundation for the development of modern control strategies.

First, equation (14) is expressed in the following matrix form:

$$\mathbf{P}_{4 \times 4} \begin{pmatrix} \ddot{\theta}_L & \ddot{\theta}_R & \ddot{\theta}_1 & \ddot{\theta}_2 \end{pmatrix}^T = \mathbf{Q}_{4 \times 10} \begin{pmatrix} \theta_L & \theta_R & \theta_1 & \theta_2 & \dot{\theta}_L & \dot{\theta}_R & \dot{\theta}_1 & \dot{\theta}_2 & u_L & u_R \end{pmatrix}^T,$$

in this representation: \mathbf{P} is a 4×4 mass-inertia matrix that groups the coefficients of the second derivatives (accelerations) of the generalized coordinates and whose structure reflects the inertial coupling between the wheels, vehicle body, and pendulum; and \mathbf{Q} is a 4×10 coefficient matrix, collecting all the remaining terms that depend on positions, velocities, and control inputs.

Each entry of the matrices is defined as follows:

\mathbf{P} elements: $p_{11} = p_{22} = 1$, represent the unit coefficients for the angular accelerations of the wheels; $p_{31} = p_{32} = \frac{r}{2}(m_1 l_1 + m_2 L_1)$ indicate the influence of the wheel dynamics on the body motion; $p_{33} = m_1 l_1^2 + m_2 L_1^2 + I_1$ corresponds to the combined rotational inertia of the vehicle body; $p_{34} = p_{43} = m_2 L_1 l_2$ reflects the coupling between the body and the pendulum; $p_{41} = p_{42} = \frac{r}{2} m_2 l_2$ relate the wheel motion to the pendulum dynamics; and $p_{44} = m_2 l_2^2 + I_2$ is the total inertia of the pendulum.

Q elements: $q_{19} = 1$ and $q_{210} = 1$ represent the actuation inputs from the left and right wheel torques, respectively; and $q_{33} = (m_1 l_1 + m_2 L_1)g$ and $q_{44} = m_2 g l_2$ are the gravitational torque components acting on the body and pendulum.

This matrix formulation enables a compact representation of the system dynamics, which is crucial for converting the model into the standard state-space form and for subsequent control design. All other matrix elements not mentioned are zero elements and $u_{L,R}$ is the system input.

In this paper, the acceleration of the left and right wheels of the car is used as the input of the system. Then, we can further get:

$$\begin{pmatrix} \ddot{\theta}_L & \ddot{\theta}_R & \ddot{\theta}_1 & \ddot{\theta}_2 \end{pmatrix}^T = \mathbf{P}_{4 \times 4}^{-1} \mathbf{Q}_{4 \times 10} \begin{pmatrix} \theta_L & \theta_R & \theta_1 & \theta_2 & \dot{\theta}_L & \dot{\theta}_R & \dot{\theta}_1 & \dot{\theta}_2 & u_L & u_R \end{pmatrix}^T.$$

The following matrix partitioning method is used:

$$\mathbf{P}_{4 \times 4}^{-1} \mathbf{Q}_{4 \times 10} = \begin{pmatrix} \mathbf{a}_{4 \times 8} & \mathbf{b}_{4 \times 2} \end{pmatrix}.$$

This approach allows for the separation of the terms associated with the state variables and the control inputs. Specifically, the product $\mathbf{P}_{4 \times 4}^{-1} \mathbf{Q}_{4 \times 10}$, which results in a 4×10 matrix, is partitioned into two submatrices: $\mathbf{a}_{4 \times 8}$, grouping the coefficients related to the state vector and its derivatives, and $\mathbf{b}_{4 \times 2}$, responsible for collecting the coefficients associated with the system inputs. This decomposition facilitates the formulation of the state-space model in the standard form $\dot{\mathbf{x}} = \mathbf{A}\mathbf{x} + \mathbf{B}\mathbf{u}$.

Then, we have:

$$\begin{pmatrix} \dot{\theta}_L & \dot{\theta}_R & \dot{\theta}_1 & \dot{\theta}_2 & \ddot{\theta}_L & \ddot{\theta}_R & \ddot{\theta}_1 & \ddot{\theta}_2 \end{pmatrix}^T = \begin{pmatrix} \mathbf{0}_{4 \times 4} & \mathbf{E}_4 \\ & \mathbf{a}_{4 \times 8} \end{pmatrix} \begin{pmatrix} \theta_L \\ \theta_R \\ \theta_1 \\ \theta_2 \\ \dot{\theta}_L \\ \dot{\theta}_R \\ \dot{\theta}_1 \\ \dot{\theta}_2 \end{pmatrix} + \begin{pmatrix} \mathbf{0}_{4 \times 2} \\ \mathbf{b}_{4 \times 2} \end{pmatrix} \begin{pmatrix} u_L \\ u_R \end{pmatrix}.$$

Making $\mathbf{A} = \begin{pmatrix} \mathbf{0}_{4 \times 4} & \mathbf{E}_4 \\ \mathbf{a}_{4 \times 8} \end{pmatrix}$ and $\mathbf{B} = \begin{pmatrix} \mathbf{0}_{4 \times 2} \\ \mathbf{b}_{4 \times 8} \end{pmatrix}$, the state equation of the system is:

$$\begin{pmatrix} \dot{\theta}_L & \dot{\theta}_R & \dot{\theta}_1 & \dot{\theta}_2 & \ddot{\theta}_L & \ddot{\theta}_R & \ddot{\theta}_1 & \ddot{\theta}_2 \end{pmatrix}^T = \mathbf{A} \begin{pmatrix} \theta_L & \theta_R & \theta_1 & \theta_2 & \dot{\theta}_L & \dot{\theta}_R & \dot{\theta}_1 & \dot{\theta}_2 \end{pmatrix}^T + \mathbf{B} \begin{pmatrix} u_L \\ u_R \end{pmatrix}. \quad (15)$$

Complementarily, the output equation of the system is:

$$y = \begin{pmatrix} 1 & 0 & 0 & 0 & 0 & 0 & 0 & 0 \\ 0 & 1 & 0 & 0 & 0 & 0 & 0 & 0 \\ 0 & 0 & 1 & 0 & 0 & 0 & 0 & 0 \\ 0 & 0 & 0 & 1 & 0 & 0 & 0 & 0 \end{pmatrix} \begin{pmatrix} \theta_L & \theta_R & \theta_1 & \theta_2 & \dot{\theta}_L & \dot{\theta}_R & \dot{\theta}_1 & \dot{\theta}_2 \end{pmatrix}^T. \quad (16)$$

With the matrices \mathbf{A} and \mathbf{B} defined, and the corresponding output relation established, the dynamic behavior of the system is now fully described in the state-space framework. In this context, equations (15) and (16) together form the complete state-space representation, providing a mathematical model suitable for control design and system analysis.

3 Controller design

3.1 LQR (Linear Quadratic Regulator) Controller

The Linear Quadratic Regulator (LQR) is an optimal control strategy widely employed in the design of controllers for linear dynamic systems represented in state-space form. Its primary objective is to determine a state linear feedback optimal control law that minimizes a quadratic cost function, thereby ensuring system performance and stability. LQR enables the design of a closed-loop optimal control system that ensures improved performance indicators while maintaining a low implementation cost compared to the original system. Moreover, it is straightforward to implement and constitutes a well-established and mature technique within modern control theory (Anderson and Moore, 1989).

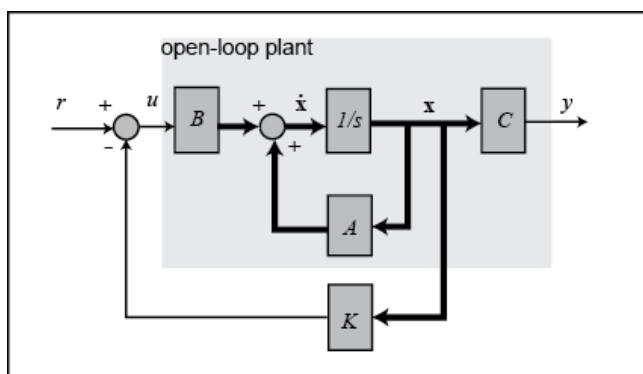
The following section provides a brief overview of the LQR principle and applies it to the stable swing process stabilization of the inverted pendulum in the self-balancing car.

Consider that the state-space expression of the continuous linear time-invariant system (assuming that the system is fully controllable) is:

$$\begin{cases} \dot{x} = \mathbf{A}x + \mathbf{B}u \\ y = \mathbf{C}x + \mathbf{D}u. \end{cases}$$

In modern control theory, the most basic control system is the full-state feedback control system, as illustrated in Figure 3). Its primary objective is to design a state feedback controller of the form $u = -\mathbf{K}x$, which represents the system's optimal control law and enables direct regulation of the system's performance through feedback from all state variables (Ogata, 2011).

Figure 3 – Full-state feedback control system



Source: <https://ctms.engin.umich.edu/CTMS>

The problem at this point is that the matrix \mathbf{K} is not unique. Thus, the question arises: what would be the best choice for \mathbf{K} ? Before introducing the cost function, consider the following analogy from the official MATLAB® tutorial: suppose you want to find the best way to get from home to work, and there are several transportation options available, such as driving, cycling, taking a bus, or renting a helicopter. Which of these options would be the best? The question itself has no definitive answer, since we have not yet defined what 'best' means. Assuming, for instance, that only time and monetary costs are considered, the information regarding the four transportation options can be shown, for illustrative and didactic purposes, in Table 2.

As observed, if minimizing time is the primary concern, renting a helicopter is the best option. On the other hand, if saving money is the priority, then riding a bicycle would be the best choice. Naturally, in real-life situations, people often seek a balance

Table 2 – Cost and money cost

Transportation	Time/min	Money/\$
Car	20	45
Bike	75	0
Bus	30	12
Helicopter	4	2578

between the two factors. For instance, if you have a morning meeting, you will likely prioritize minimizing travel time. However, if your budget is limited, financial cost will also be an important consideration. In this case, how can we make an informed choice? A straightforward approach is to use a simple quantitative evaluation method by defining an evaluation function of the form $J = \mathbf{Q} \cdot \text{Time} + \mathbf{R} \cdot \text{Money}$. This function allows assigning different weights to time and monetary costs based on individual preferences or priorities. If the weighting parameters are defined as in Table 3, driving becomes the most favorable option for going to work. On the other hand, when the weights are set as shown in Table 4, taking the bus becomes the best alternative.

Table 3 – Example Cost Function 1

Transportation	Q	Time/min	R	Money/\$	J(Cost)
Car	10	20	1	45	245
Bike	10	75	1	0	750
Bus	10	30	1	12	312
Helicopter	10	4	1	2578	2618

Table 4 – Example Cost Function 2

Transportation	Q	Time/min	R	Money/\$	J(Cost)
Car	10	20	1	45	325
Bike	10	75	1	0	375
Bus	10	30	1	12	210
Helicopter	10	4	1	2578	12910

Similarly, in the context of control systems, a cost function, specifically, a Quadratic Cost Function, is introduced to evaluate system performance, as shown in Equation (17) below:

$$J = \int_0^{+\infty} \left[x^T(t) \mathbf{Q} x(t) + u^T(t) \mathbf{R} u(t) \right] dt, \quad (17)$$

where: \mathbf{Q} is the state weighting matrix, which is semi-positive definite and assigns relative importance to each state variable in the cost function, allowing certain states to be penalized more heavily based on their impact on system performance; \mathbf{R} is the control weighting matrix, which is positive definite and determines the penalty associated with the control inputs, effectively penalizing overly aggressive or energy-intensive control actions.

In engineering practice, both \mathbf{Q} and \mathbf{R} are typically symmetric and often chosen to be diagonal matrices, simplifying their implementation and interpretation. The diagonal elements q_i of \mathbf{Q} represent the relative importance of the error associated with the corresponding state variable x_i . Similarly, the diagonal elements r_i in \mathbf{R} represent the restrictions, or penalties, on the corresponding input component u_i , ensuring that their magnitudes remain within acceptable limits.

Since the goal of the optimal control strategy is to drive all state variable to zero, each state value is treated as an error to be minimized, called the error value. The greater the importance of a given error component, the more rapidly it is expected to diminish. Consequently, a larger weighting coefficient is assigned to emphasize its reduction in the control strategy. The design principle of the LQR controller is to construct a state feedback law $u = -\mathbf{K}x$ that minimizes the cost function $\min J$. The objective is to ensure improved performance of the original system, achieving better performance indicators, while keeping the control effort economically efficient.

Regarding the computation of the state feedback matrix \mathbf{K} , only the final results are presented here, without detailing the intermediate steps, which can be observed below:

$$\mathbf{K} = \mathbf{R}^{-1}\mathbf{B}^T\mathbf{P},$$

where, \mathbf{P} is the solution of the Ricatti equation, which is show below:

$$\mathbf{A}^T\mathbf{P} + \mathbf{P}\mathbf{A} + \mathbf{Q} - \mathbf{P}\mathbf{B}\mathbf{R}^{-1}\mathbf{B}^T\mathbf{P} = \mathbf{0}.$$

Similarly, for a discrete linear time-invariant system (assuming that the system is

completely controllable), the state equation can be expressed as:

$$x(k+1) = \mathbf{A}x(k) + \mathbf{B}u(k),$$

the quadratic performance index is given by:

$$J = \sum_0^{+\infty} \left[x^T(k) \mathbf{Q} x(k) + u^T(k) \mathbf{R} u(k) \right] dt,$$

where: \mathbf{Q} is a symmetric positive definite constant matrix or a symmetric semi-positive definite constant matrix, which penalize the states; and \mathbf{R} is a symmetric positive definite constant matrix, which penalize the control effort.

The objective is to design a state feedback controller $u(k) = -\mathbf{L}x(k)$ that J is minimized. As in the previous case, only the key results are presented here.

$$\mathbf{L} = (\mathbf{R} + \mathbf{B}^T \mathbf{P} \mathbf{B})^{-1} \mathbf{B}^T \mathbf{P} \mathbf{A},$$

where, \mathbf{P} is the solution of the Ricatti equation, which is show below:

$$\mathbf{Q} - \mathbf{P} + \mathbf{A}^T \mathbf{P} \mathbf{A} - \mathbf{A}^T \mathbf{P} \mathbf{B} (\mathbf{R} + \mathbf{B}^T \mathbf{P} \mathbf{B})^{-1} \mathbf{B}^T \mathbf{P} \mathbf{A} = 0.$$

3.2 Application Example

With the qualitative overview of the LQR controller provided above, the next step is to demonstrate its design through the stabilization of an inverted pendulum on a self-balancing cart. This example serves to illustrate the practical application of the LQR design methodology.

First define the parameters of the inverted pendulum on a balancing cart:

$$m_1 = 0.9, m_2 = 0.1, r = 0.0335, L_1 = 0.126, L_2 = 0.390, l_1 = \frac{L_1}{2}, l_2 = \frac{L_2}{2}, g = 9.8, I_1 = \left(\frac{1}{12}\right) \cdot m_1 \cdot L_1^2 \text{ and } I_2 = \left(\frac{1}{12}\right) \cdot m_2 \cdot L_2^2.$$

Substituting the values and after applying the matrix partitioning method, we have:

$$\begin{pmatrix} \dot{\theta}_L \\ \dot{\theta}_R \\ \dot{\theta}_1 \\ \dot{\theta}_2 \\ \ddot{\theta}_L \\ \ddot{\theta}_R \\ \ddot{\theta}_1 \\ \ddot{\theta}_2 \end{pmatrix} = \underbrace{\begin{bmatrix} 0 & 0 & 0 & 0 & 1 & 0 & 0 & 0 \\ 0 & 0 & 0 & 0 & 0 & 1 & 0 & 0 \\ 0 & 0 & 0 & 0 & 0 & 0 & 1 & 0 \\ 0 & 0 & 0 & 0 & 0 & 0 & 0 & 1 \\ 0 & 0 & 0 & 0 & 0 & 0 & 0 & 0 \\ 0 & 0 & 0 & 0 & 0 & 0 & 0 & 0 \\ 0 & 0 & 131.6239 & -17.9487 & 0 & 0 & 0 & 0 \\ 0 & 0 & -63.7870 & 46.3905 & 0 & 0 & 0 & 0 \end{bmatrix}}_A \begin{pmatrix} \theta_L \\ \theta_R \\ \theta_1 \\ \theta_2 \\ \dot{\theta}_L \\ \dot{\theta}_R \\ \dot{\theta}_1 \\ \dot{\theta}_2 \end{pmatrix} + \underbrace{\begin{bmatrix} 0 & 0 \\ 0 & 0 \\ 0 & 0 \\ 0 & 0 \\ 1 & 0 \\ 0 & 1 \\ -0.1943 & -0.1943 \\ 0.0297 & 0.0297 \end{bmatrix}}_B \begin{pmatrix} u_L \\ u_R \end{pmatrix},$$

and the output equation of the system is:

$$y = \underbrace{\begin{pmatrix} 1 & 0 & 0 & 0 & 0 & 0 & 0 & 0 \\ 0 & 1 & 0 & 0 & 0 & 0 & 0 & 0 \\ 0 & 0 & 1 & 0 & 0 & 0 & 0 & 0 \\ 0 & 0 & 0 & 1 & 0 & 0 & 0 & 0 \end{pmatrix}}_C \begin{pmatrix} \theta_L & \theta_R & \theta_1 & \theta_2 & \dot{\theta}_L & \dot{\theta}_R & \dot{\theta}_1 & \dot{\theta}_2 \end{pmatrix}^T.$$

The matrix $D = \mathbf{0}_{4 \times 2}$.

For the design of the LQR controller, a sampling period of 0.01 is used to discretize the system and relevant MATLAB® functions are used.

The Q and R matrices used were respectively:

$$Q = \begin{bmatrix} 51.2938 & 0 & 0 & 0 & 0 & 0 & 0 & 0 \\ 0 & 51.2938 & 0 & 0 & 0 & 0 & 0 & 0 \\ 0 & 0 & 32.8281 & 0 & 0 & 0 & 0 & 0 \\ 0 & 0 & 0 & 131.3123 & 0 & 0 & 0 & 0 \\ 0 & 0 & 0 & 0 & 51.2938 & 0 & 0 & 0 \\ 0 & 0 & 0 & 0 & 0 & 51.2938 & 0 & 0 \\ 0 & 0 & 0 & 0 & 0 & 0 & 131.3123 & 0 \\ 0 & 0 & 0 & 0 & 0 & 0 & 0 & 131.3123 \end{bmatrix},$$

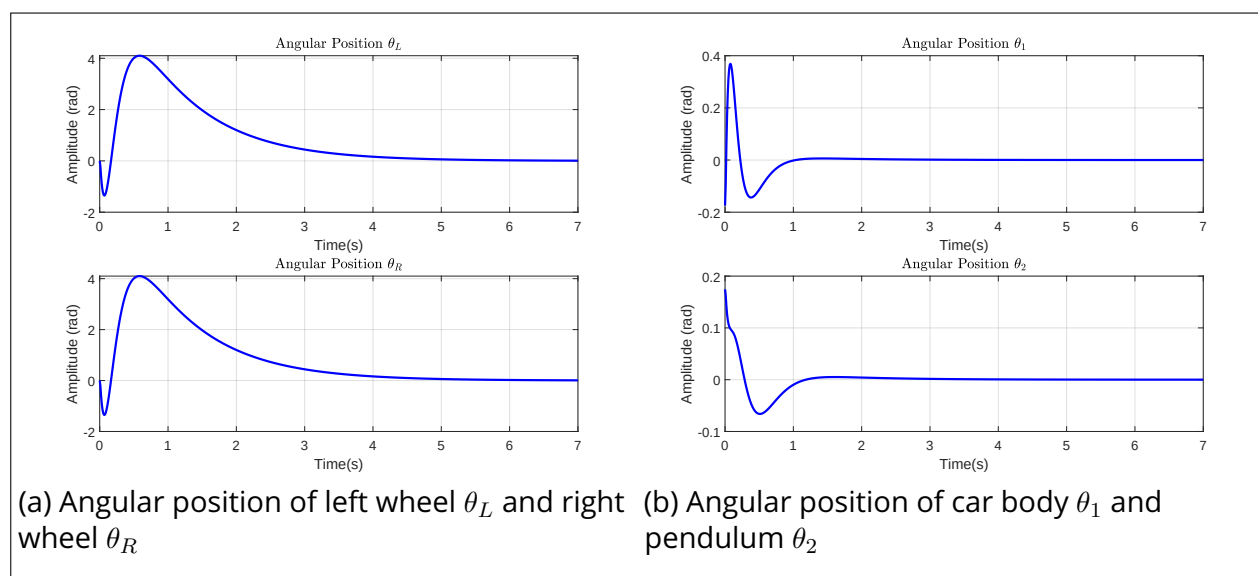
$$R = 0.0005 \cdot \begin{bmatrix} 1 & 0 \\ 0 & 1 \end{bmatrix}.$$

The initial conditions are defined as: $x_0 = \begin{bmatrix} 0 & 0 & -0.1745 & 0.1745 & 0 & 0 & 0 & 0 \end{bmatrix}^T$ and the gains found in the stabilization design were:

$$K = \begin{bmatrix} 81.26 & -10.06 & 5492.40 & 18921.70 & 100.36 & 8.03 & 447.30 & 2962.77 \\ 81.26 & -5492.40 & 18921.70 & 8.03 & 100.36 & 447.30 & 2962.77 & 10.06 \end{bmatrix}. \quad (18)$$

Applying the control law $u = -Kx$, with K defined in Equation 18, the closed-loop system presented satisfactory performance, which is shown in Figure 4.

Figure 4 – Discrete Time System LQR Simulations Results



Source:Authors, May 2025

The graphics in Figure 4 illustrate the system's behavior under the designed LQR controller. The subfigures (a) and (b) show the angular positions of the system's components over time. As observed, the angles θ_1 and θ_2 converge rapidly to zero, indicating that both the cart body and the pendulum are successfully stabilized around the upright equilibrium position. The responses exhibit minimal overshoot and no sustained oscillations, confirming that the controller ensures a fast and smooth settling

behavior. These results support the theoretical predictions and demonstrate the practical viability of the LQR approach for stabilizing nonlinear, underactuated systems in discrete time.

4 CONCLUSIONS

Throughout this work, a comprehensive mathematical model of the nonlinear dynamic system, the inverted pendulum on a self-balancing cart, was developed, capturing the system's essential physical characteristics and interactions. This was followed by a linearization process that enabled the formulation of an appropriate state-space representation, serving as the foundation for control system design. Based on this linear model, the theoretical foundations of the Linear Quadratic Regulator (LQR) controller were thoroughly presented, including the formulation of the cost function and the interpretation of the weighting matrices. With this foundation, the design of the LQR controller was carried out with the objective of stabilizing the system around its unstable equilibrium point. Simulation results validated the effectiveness of the proposed controller, as can be observed in Figure 4, demonstrating its ability to regulate the system even under adverse conditions such as disturbances and varied initial states. Consequently, the successful validation of the LQR controller also confirms the precision and reliability of the system's mathematical model. The controller provided a fast response with minimal oscillations and high precision in maintaining the pendulum's upright position, thereby highlighting the LQR's ability to optimize system performance by balancing state error and control effort through cost function minimization, which successfully reached the expected result.

ACKNOWLEDGEMENTS

The authors would like to thank the editorial team of the *Ciência e Natura* journal for their support and the opportunity to publish this scientific paper. The authors also acknowledge the organizers of the 3rd Science, Technology and Innovation Fair of the Federal University of Santa Maria, Cachoeira do Sul Campus, for providing a valuable space for academic dissemination and for the opportunity to present and share this study in such an enriching environment.

REFERENCE

- Alves, G. O. (2017). *Mecânica lagrangiana e hamiltoniana*. Self-published. Retrieved from <https://github.com/gabrielocalves/mecanica-lagrangiana>.
- Anderson, B. D. O. & Moore, J. B. (1989). *Optimal control: Linear quadratic methods*. Prentice Hall, Englewood Cliffs, NJ.
- Anderson, C. W. (1989). Learning to control an inverted pendulum using neural networks. *IEEE Control Systems Magazine*, 9(3):31–37.
- Åström, K. J. & Furuta, K. (2000). Swinging up a pendulum by energy control. *Automatica*, 36(2):287–295.
- Bugeja, M. (2003). Non-linear swing-up and stabilizing control of an inverted pendulum system. In *The IEEE Region 8 EUROCON 2003. Computer as a Tool*, volume 2, pages 437–441, Antalya, Turkey.
- Chen, Y.-F. & Huang, A.-C. (2014). Adaptive control of rotary inverted pendulum system with time-varying uncertainties. *Dynamics*, 76:95–102.
- Eini, R. & Abdelwahed, S. (2019). Indirect adaptive fuzzy model predictive control of a rotational inverted pendulum. <https://arxiv.org/abs/1903.07645>. [Preprint]. arXiv.
- Huang, S.-J. & Huang, C.-L. (1994). Control of an inverted pendulum using grey prediction model. In *Proceedings of 1994 IEEE Industry Applications Society Annual Meeting*, volume 2, pages 1936–1941, Phoenix, AZ, USA.
- Kumar, E. V. & Jerome, J. (2013). Robust lqr controller design for stabilizing and trajectory tracking of inverted pendulum. *Procedia Engineering*, 64:169–178. International Conference on Design and Manufacturing (IConDM2013).
- Lynch, K. M. & Park, F. C. (2017). *Modern robotics*. Cambridge University Press, Cambridge, UK.

Nise, N. S. (2013). *Engenharia de sistemas de controle*. LTC, Rio de Janeiro, RJ, 6 edition. Translation and technical review by J. P. Matsuura.

Ogata, K. (2011). *Engenharia de controle moderno*. Pearson Prentice Hall, Upper Saddle River, NJ, 5 edition. Translation by H. C. de Souza & E. A. Tannur.

Santos, T. F. d. S. (2022). Estudo de técnicas de controle aplicadas ao problema de estabilização de um pêndulo invertido. Bachelor's thesis, Universidade Tecnológica Federal do Paraná.

Stimac, A. K. (1999). *Standup and stabilization of the inverted pendulum*. Doctoral dissertation, Massachusetts Institute of Technology.

Taylor, J. R. (2005). *Classical mechanics*. University Science Books, Sausalito, CA.

Author contributions

1 – Pedro Henrique Cascardo Cabral

Undergraduate student in Electrical Engineering course, Federal University Of Santa Maria - Cachoeira do Sul

<https://orcid.org/0009-0003-9168-3635> • pedrohcascardoc@gmail.com

Contribution: Conceptualization; Methodology; Writing – Original Draft Preparation

2 – André F. Caldeira (Corresponding Author)

PhD in Electrical Engineering, Professor of the Electrical Engineering course, Federal University of Santa Maria - Cachoeira do Sul.

<https://orcid.org/0000-0002-4939-2709> • andre.caldeira@ufsm.br

Contribution: Conceptualization, Literature Review, Methodology, Data Analysis, Writing – Original Draft Preparation

3 – Charles Rech

PhD in Mechanical Engineering, Professor of the Mechanical Engineering course, Federal University of Santa Maria - Cachoeira do Sul.

<https://orcid.org/0000-0001-8523-6300> • charles.rech@ufsm.br

Contribution: Conceptualization, Literature Review, Methodology, Data Analysis, Writing – Review & Editing

4 – Simone F. Venturini

MSc in Mechanical Engineering, PhD student in the postgraduate program in production engineering PPGE-UFMS, Santa Maria, RS.

<https://orcid.org/0000-0002-9439-0008> • simone.venturini@ufsm.br

Contribution: Conceptualization; Methodology; Writing – Review & Editing

5 – Cristiano F. Maidana

PhD in Mechanical Engineering, Professor of the Mechanical Engineering course, Federal University of Santa Maria - Cachoeira do Sul.

<https://orcid.org/0000-0003-3137-6177> • cristiano.maidana@ufsm.br

Contribution: Conceptualization, Methodology, Data Analysis, Writing – Review & Editing

6 – Carmen Brum Rosa

PhD in Electrical Engineering, Professor in the Posgraduate Program in Production Engineering (PPGEP), Federal University of Santa Maria - Santa Maria

<https://orcid.org/0000-0002-0173-081X> • carmen.b.rosa@ufsm.br

Contribution: Conceptualization, Writing – Review & Editing

How to cite this article

Cabral, P. H. C., Caldeira, A. F., Rech, C., Venturini, S. F., Maidana, C. F. & Rosa, C. B. (2025) Stabilization control of the inverted pendulum on a self-balancing cart, *Ciência e Natura*, Santa Maria, n. spe. 4, e92195. <https://doi.org/10.5902/2179460X92185>